IEEE Access
Multidisciplinary ⋮ Rapid Review ⋮ Open Access Journal

Received 29 July 2023, accepted 6 August 2023, date of publication 14 August 2023, date of current version 30 August 2023.

Digital Object Identifier 10.1109/ACCESS.2023.3304694

RESEARCH ARTICLE

Dipole Array Sensor for Microwave Breast Cancer Detection

MAGED A. ALDHAEEBI, (Member, IEEE), AND THAMER S. ALMONEEF, (Member, IEEE)
Electrical Engineering Department, College of Engineering, Prince Sattam bin Abdulaziz University, Al-Kharj 11942, Saudi Arabia

Corresponding author: Thamer S. Almoneef (t.almoneef@psau.edu.sa)

This work was supported by Prince Sattam bin Abdulaziz University through the Deputyship for Research and Innovation, Ministry of Education in Saudi Arabia, under Project IF-PSAU-2021/01/17697.

ABSTRACT In this paper, a novel design of a near-field dipole antenna sensor array for breast tumor detection is presented. The proposed sensor consists of four electrically small dipole antennas fed by a single port. Due to the proven fact that breast tumors have higher dielectric properties than the surrounding normal tissues, the proposed sensor is utilized for detecting breast tumors by evaluating the variations of the sensor's response of two cases, normal and abnormal, of the breast tissues. A simulation study is performed using both normal and abnormal numerical breast phantoms with different sizes of tumors inserted at different locations. Simulation results show the proposed sensor detected the inserted tumors at various locations inside the normal breast phantom due to an increased area of sensitivity of the sensor by using multiple sensors array. An experimental study is conducted on breast chicken meat that mimics a healthy breast and two cases of tumors including tumors made of oil and gelatin mixture and conductive spheres with different sizes inserted at different locations inside the chicken meat. Experimental results show that the proposed sensor has higher sensitivity for detecting different sizes of breast tumors placed at multiple locations.

INDEX TERMS Near-field, microwave sensors, sensor array, microwave detection, breast tumor.

I. INTRODUCTION

Microwave, imaging (MI) techniques has gained great interest from the researchers for breast cancer detection due to some advantages over current techniques, such as MRI, ultrasound, and X-ray mammography for breast tumor detection. Such advantages include non-ionizing, inexpensive, non-invasive, and comfortably used by patients [1]. Moreover, MI does not use ionizing radiation, is noninvasive and safe, and can be repeated for several testing without any impacts for patient's health. The fundamental key behind using MI for breast tumor detection is that the breast tumor tissues have higher dielectric properties than normal tissues in the microwave frequencies band [1], [2], [3], [4], [5], [6].

MI system consists of two major sections for detecting breast tumors hardware and software. The fundamental part of the hardware section is the microwave sensors that send microwave signals to the breast tissues and receive them back [1], [2], [3], [7]. Therefore, the accuracy of MI in detecting breast tumors is almost based on the performance of the microwave sensors [7]. In the literature, several types of microwave sensors are utilized for designing MI systems, which are based on conventional antenna, such as patch, monopole, loop, horn, dipole, and Vivaldi [1], [2], [3], [4], [5], [6], [7], [8], [9], [10], [11], [12], [13], [14].

Designing MI systems for breast tumor detection is usually based on two configurations of microwave sensors including signal and array sensors [1], [2], [3], [4], [5], [6], [7], [8], [9], [10], [11], [12], [13], [14], [15]. Developing MI systems based on a single sensor structure makes the testing more complicated and takes much time due to the use of motorized scanning to acquire information from multiple projections and angles of the breast tissues, which results in low accuracy of the MI system [1], [2], [3], [4], [5], [6], [7], [8], [9], [10], [11], [12], [13], [14], [15], [16], [17], [18], [19], [20], [21]. On the other hand, array sensors are used with multiple feeds

The associate editor coordinating the review of this manuscript and approving it for publication was Wen-Sheng Zhao.

to get information from several positions around the breast tissues, which leads to a complex, enormous, and costly system [18], [22], [23], [24], [25], [26], [27], [28], [29].

In the previous studies [20], [21] single dipole and loop antennas were designed as near-field microwave sensors to detect breast tumors of various sizes at different locations by using scanning methodology. In both studies, the performance of the developed microwave sensors and detection system is based on the different values of either magnitude or phase of the reflection coefficient of both testing of the right and the left breasts that are symmetrical in shape and content.

Both studies show that using a dipole sensor provide more sensitivity for detecting high dielectric materials than the loop sensor, on other hand, the loop sensor is more highly sensitive to conductive materials than the dipole sensor. The physical explanation behind this concluded that the dominant field in the dipole sensor is the electric field whereas the magnetic field is considered the dominant field in the loop sensor. In another study [29], an array loop sensor feds by a single port is developed to improve the sensitivity of the microwave detection system for the detection of metallic spheres that mimic high conductive breast tumors.

In this paper, electrically small four dipole antenna arrays excited by a single port proposed as a microwave sensor for near-field microwave breast tumor detection is presented. As mentioned at the beginning of this introduction that breast tumors exhibit higher electrical properties than normal tissues. Moreover, the ratio of the dielectric properties in the difference between breast tumors and normal tissues is higher than the conductive properties. The proposed dipole array sensor will have higher sensitivity for detecting the of breast tumors due to the improvement of the sensitivity area as compared to the single sensor as proven in the previous study using loop array sensor in [29].

The proposed sensor is used for microwave detection of breast tumors based on the fact that both breasts (right and left) of a female human are symmetric in material tissues composition [30], [31]. The testing method uses dual sensors simultaneously with the right and left breasts. Then, the reflection coefficient responses of the two sensors are recorded and analyzed to check for any abnormality in one of the breasts. If the response of the two sensors are different, that indicates the presence of a tumor in one of the breasts otherwise both breast are healthy.

II. SIMULATION AND SENSOR ARRAY DESIGN

The overall size of the presented sensor array is L = 123 mm × W = 30 mm, comprising of four electrically small printed dipole arrays. All four electrically small dipoles have identical length ld and width wd of 30 mm and 3 mm respectively. These electrically small dipoles are printed in top of RO4003C substrate material with thickness of 1.52 mm. The top layer is connected with the bottom layer using 1 mm vias through each gap between the two arms of the electrically small dipole. These vias are connected to

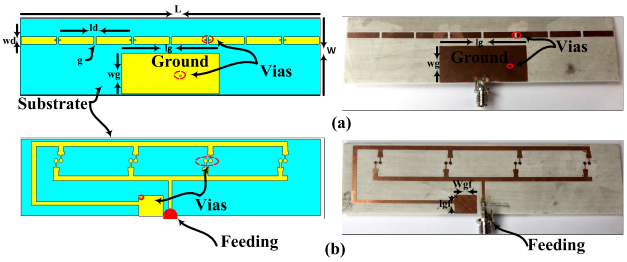

FIGURE 1. The presented array dipole sensor. (a) showing the top layer that includes the electrically small dipole elements array. (b) showing the bottom layer that includes the feed networks.

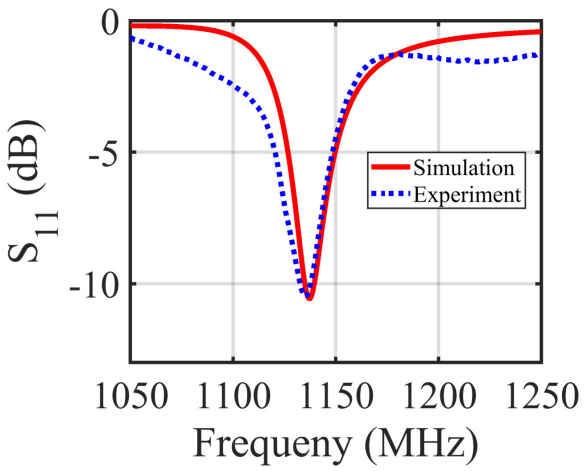

FIGURE 2. Demonstrating the S_{11} of the introduced sensor array in: (a) CST simulation and (b) measurement result of fabricated sensor.

each dipole to a bottom-ground layer that contains a single port feeding network and shared ground of lg = 40 mm and Wg = 17 mm placed on the top layer shown in Fig. 1(a). Each microstrip line of the feeding network is optimized to distribute the exciting signal equally to all electrically small dipoles and operate at the resonance frequency of 1130 MHz using the optimization logarithms in CST [32] software as illustrated in Fig. 1(b). The optimized sensor array was manufactured as shown in Fig. 1. The reflection coefficient response of both simulated and measured sensors are in strong agreement as demonstrated in Fig. 2

Next step in the simulation section, a numerical breast phantom model of the ID: 062204 ACR classification: Class No 3 is developed and imported into CST as introduced in [21], [32], [33], [34], and [35]. The developed breast phantom model is simulated with the proposed sensor to analyze the sensitivity of the proposed sensor for detecting breast tumors inserted at any location inside the breast model without a scanning mechanism at three different distances off between the sensor and the breast phantom model as explained in the following simulations studies.

In the first simulation, the sensor is simulated with the normal numerical breast phantom at a stand-off distance of 5 mm between the phantom and the sensor as shown in Fig. 3 (a). Next step, the array sensor's response was

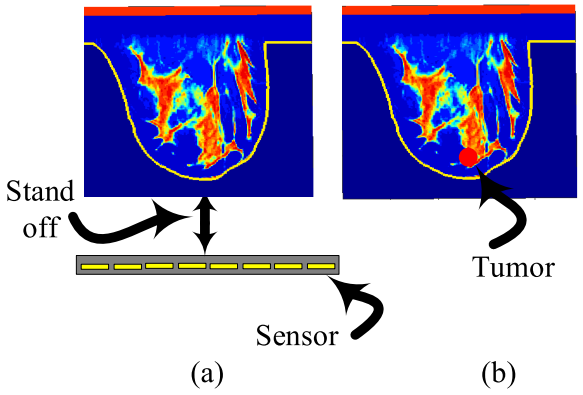

FIGURE 3. Illustrating the configuration of simulation modeling: (a) showing the normal numerical breast phantom with the presented array dipole sensor placed at a 5mm stand-off distance away from the phantom. (b) showing the abnormal breast phantom which contains a breast tumor.

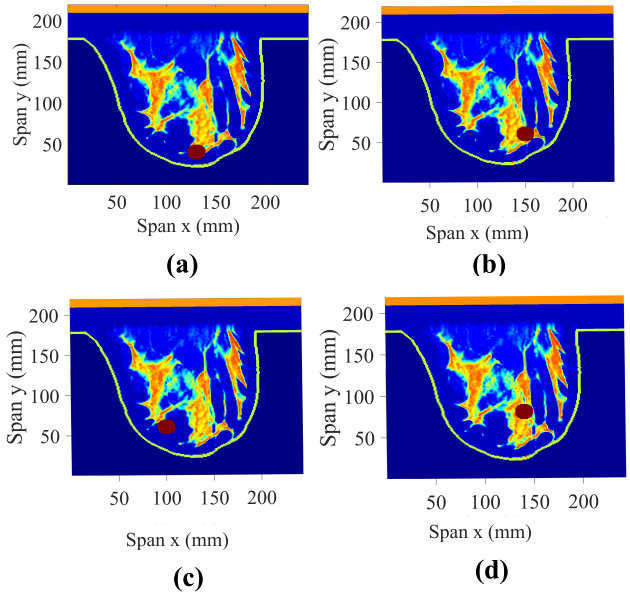

FIGURE 4. Simulation setup of four different tumor locations inside the normal breast phantom model. A 10 mm breast tumor is inserted at four different random locations inside the breast tissues. (a) Tumor located at L1 (x = 130 mm, y = 40 mm, z = 140 mm). (b) Tumor located at L2 (x = 150 mm, y = 60 mm, z = 140 mm). (c) Tumor located at L3 (x = 140 mm, y = 90 mm, z = 140 mm). (d) Tumor located at L4 (x = 150 mm, y = 90 mm, z = 140 mm).

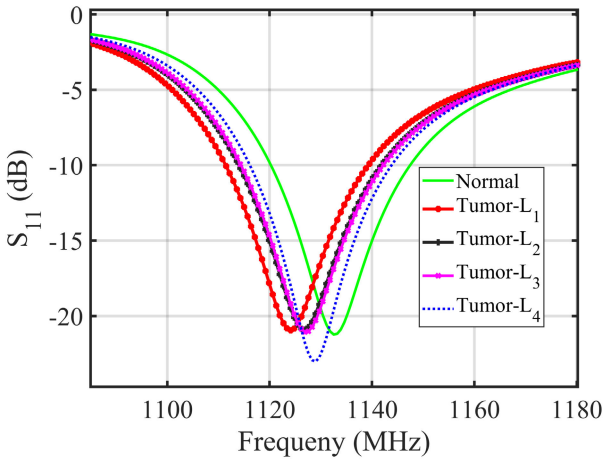

FIGURE 5. Presented the simulation results of the sensor's S_{11} magnitude response of both simulations studies of a normal phantom without tumor and an abnormal phantom containing a 10 mm tumor, at four various locations at stand off distance of 5 mm.

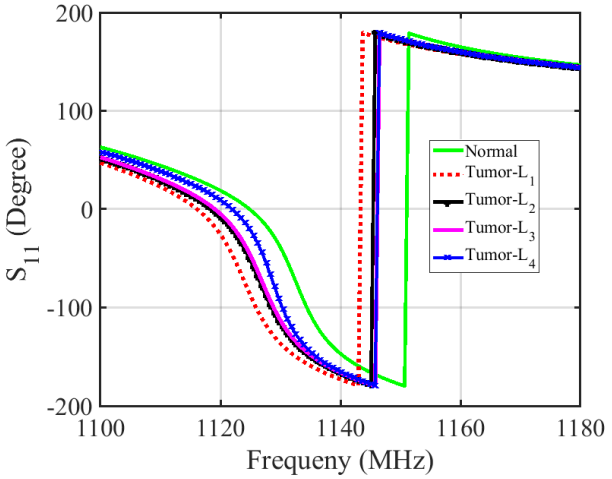

FIGURE 6. Presented the simulation results of the sensor's S_{11} phase response of both simulations studies of a normal phantom without tumor and an abnormal phantom containing a 10 mm tumor, at four various locations at stand off distance of 5 mm.

recorded, which included the data of the reflection coefficient magnitude and phase changes with frequency. Next, the designed sensor was then simulated four times separately with an abnormal breast phantom at the same stand-off distance of 5 mm, where the tumor of 10 mm inserted at four various locations L1, L2, L3, and L4 as shown in Fig. 4.

The array sensor reflection coefficient of the four various simulation of the four locations were then recorded. Finally, the simulated data of both normal phantom and abnormal phantoms, which includes the phase and the magnitude of the sensor's reflection coefficient were analyzed to detect the presence of the tumor.

The collecting data of the sensor response from both normal and abnormal simulations, normal phantom without tumor and abnormal phantoms with inserted tumor at four locations is analyzed as shown in Fig. 5 and Fig. 6. Figure 5 and Fig. 6 show the sensor magnitude response S_{11}, and the phase response of S_{11} respectively.

As results show noticeable differences in sensor responses, magnitude, and phase, of both simulation studies, normal and abnormal phantoms, it is evident from these results that the sensor is highly sensitive having the ability to distinguish between healthy and non-healthy breasts. The sensor sensitivity is higher at the tumor inserted close to it than at the other locations. The sensitivity refers here to the highest shift in magnitude and phase of the S_{11} of the sensor compared to the normal case.

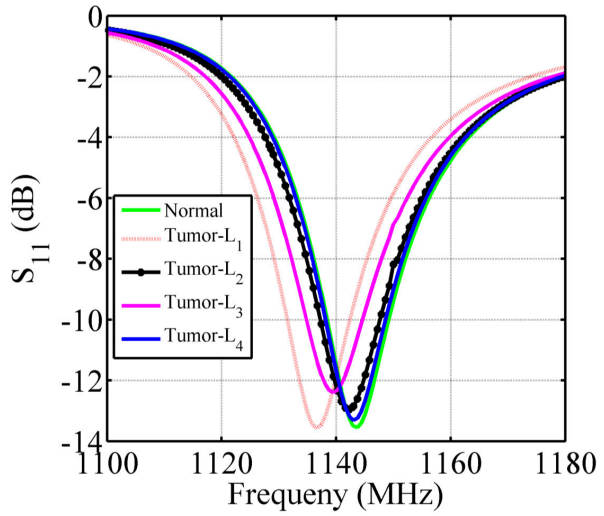

FIGURE 7. Presented the simulation results of the sensor's S_{11} magnitude response of both simulations studies of a normal phantom without tumor and an abnormal phantom containing a 10 mm tumor, at four various locations at stand off distance of 10 mm.

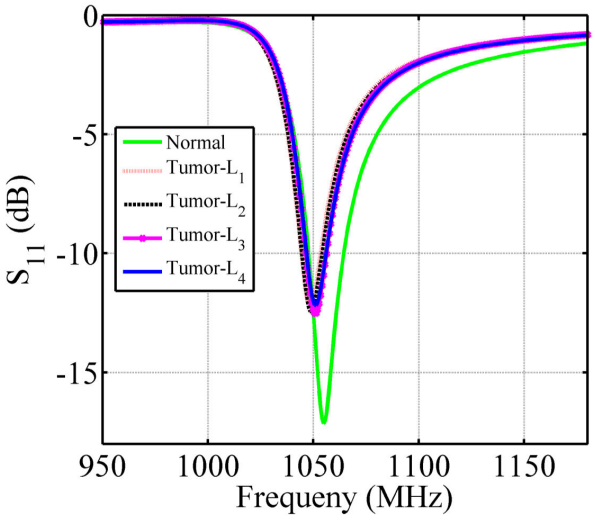

FIGURE 9. Presented the simulation results of the sensor's S_{11} magnitude response of both simulations studies of a normal phantom without tumor and an abnormal phantom containing a 10 mm tumor, at four various locations at stand off distance of 15 mm.

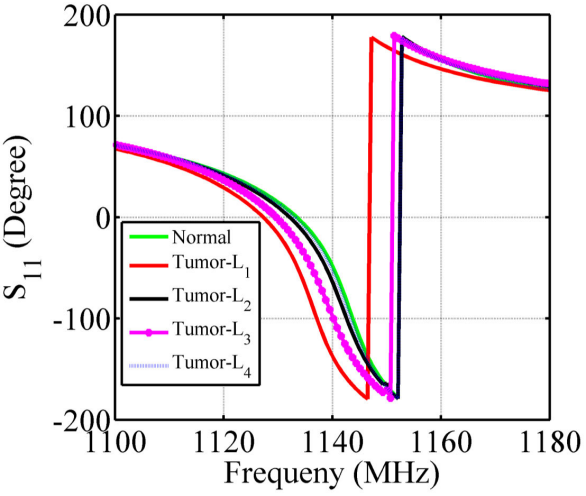

FIGURE 8. Presented the simulation results of the sensor's S_{11} phase response of both simulations schemes of a normal phantom without tumor and an abnormal phantom containing a 10 tumor, at four various locations at stand off distance of 10 mm.

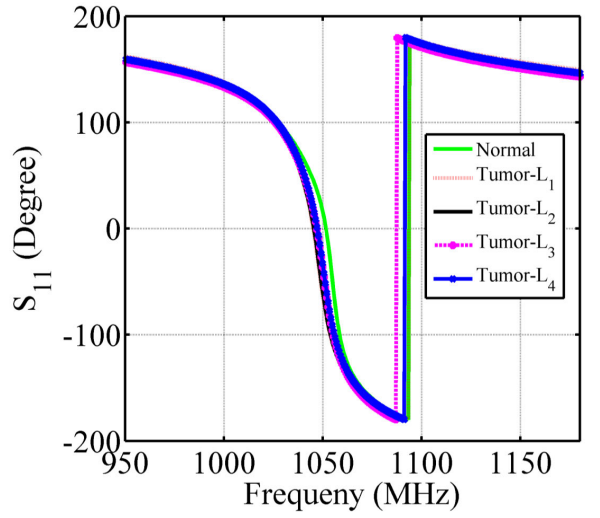

FIGURE 10. Presented the simulation results of the sensor's S_{11} phase response of both simulations studies of a normal phantom without tumor and an abnormal phantom containing a 10 mm tumor, at four various locations at stand off distance of 15 mm.

In the second simulation study, the sensor is simulated with normal and abnormal breast phantoms model at a stand-off distance of 10 mm.The same process are done regrading collecting data as the first simulation study.

The simulation results of the sensor response with normal and abnormal phantoms at a distance off of 10 mm are shown in Fig. 7 and Fig. 8 which show the sensor magnitude response S_{11}, and the phase response of S_{11} respectively.

Similarly, in the third simulation study, the sensor is simulated with normal and abnormal breast phantoms model at a stand-off distance of 15 mm.The same process are done regrading the collecting data as the first and second simulation study.

The simulation results of the sensor response with normal and abnormal phantoms at a distance off of 15 mm are shown in Fig. 9 and Fig. 10 highlighting the sensor magnitude response S_{11}, and the phase response of S_{11} respectively.

As results show noticeable differences in sensor responses, magnitude, and phase, of both simulation studies, normal and abnormal phantoms, evidence from these results indicate that the sensor is sensitive to differentiate between healthy and non-healthy breasts. The sensor sensitivity is higher at locations of the tumor closer to the sensor than at the other locations. Moreover, the sensor sensitivity is higher at a distance off of 5 mm when compared to a distance off of 10mm and 15 mm. Therefore, we can conclude that the closer the sensor to the breast phantom the more sensitive the sensor is due to the higher interaction between the magnetic and electric fields of the sensor with the breast phantom.

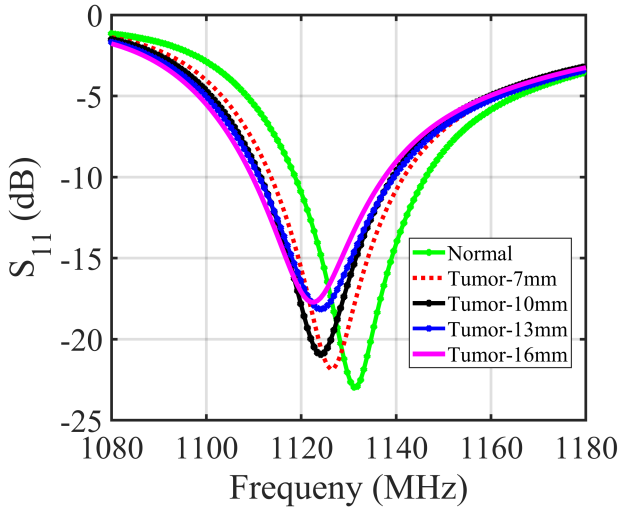

FIGURE 11. Presented the simulation results of the sensor's S_{11} magnitude response of the simulations studies that simulate four different sizes of tumor (7 mm,10 mm, 13 mm, and 16 mm) placed at the same location inside a normal breast phantom.

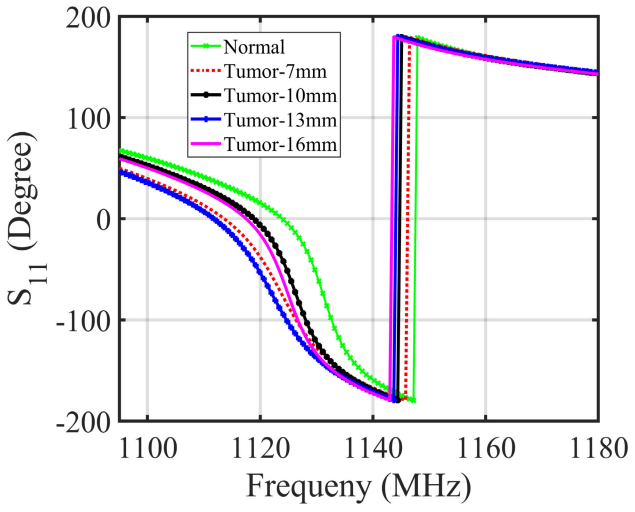

FIGURE 12. Presented the simulation results of the sensor's S_{11} phase response of the simulations studies that simulate four different sizes of tumor (7 mm,10 mm, 13 mm, and 16 mm) placed at the same location inside a normal breast phantom.

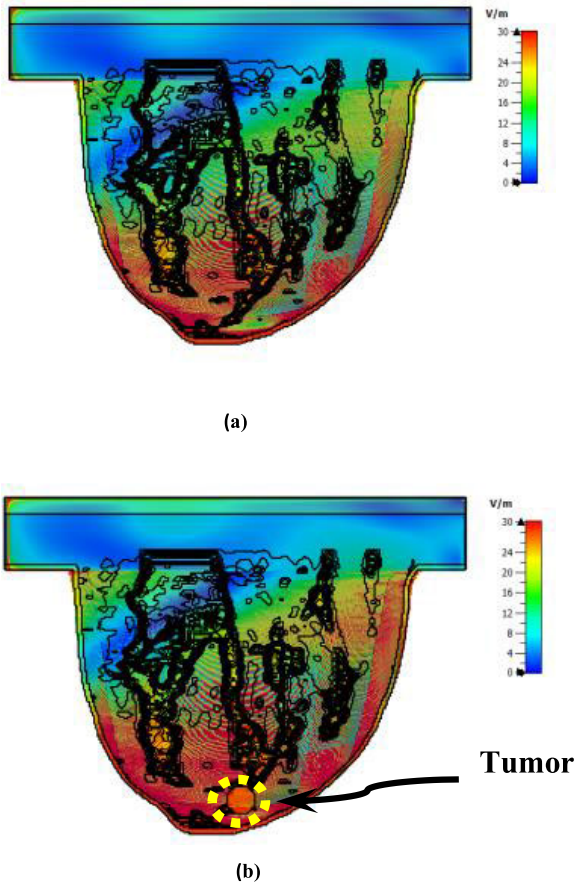

FIGURE 13. Shows electric field distribution inside: (a) healthy breast model, and (b) Non-healthy breast model containing a 10 mm tumor.

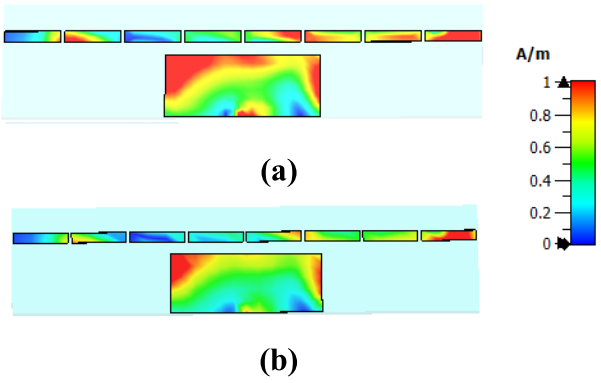

FIGURE 14. Shows electric field distribution inside: (a) healthy breast model, and (b) Non-healthy breast model containing a 10 mm tumor.

To validate the sensitivity performance of the presented sensor, another simulation study was conducted for detecting four different sizes of breast tumors, in an early stages with size less than 2 cm and have not yet spread deeply into the chest wall [36] including 7 mm, 10 mm, 13 mm, and 16 mm, of breast tumors, inserted in a fixed location inside a healthy breast phantom as shown in Fig. 3(b).

Noticeably from the showing results, of both magnitude and phase, the sensitivity of the sensor for detecting large tumors sizes is higher than the smaller ones as shown in Fig. 11 and Fig. 12

Figure. 13 shows electric field distributions in normal and abnormal breast phantoms. The obtained results demonstrate that the electric field intensity is more confined and distributed inside the abnormal breast in the surrounding region of the tumor than the normal breast model due to the fact that the abnormal breast which contains a tumor has a higher permittivity and conductivity than the normal breast model.

Figure. 14 shows surface current distributions of the proposed sensor simulated with both normal and abnormal breast phantoms. The results show that the surface current of the proposed sensor simulated with normal breast phantom model is different than the surface current of the sensor in

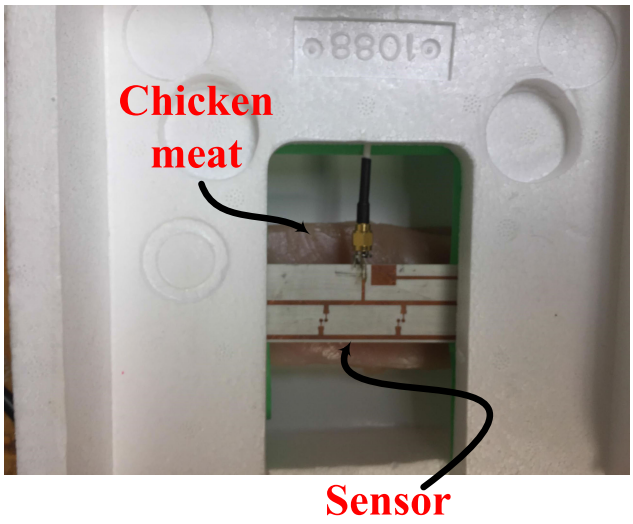

FIGURE 15. Measurement setup showing the proposed dipole array sensor with a chicken meat.

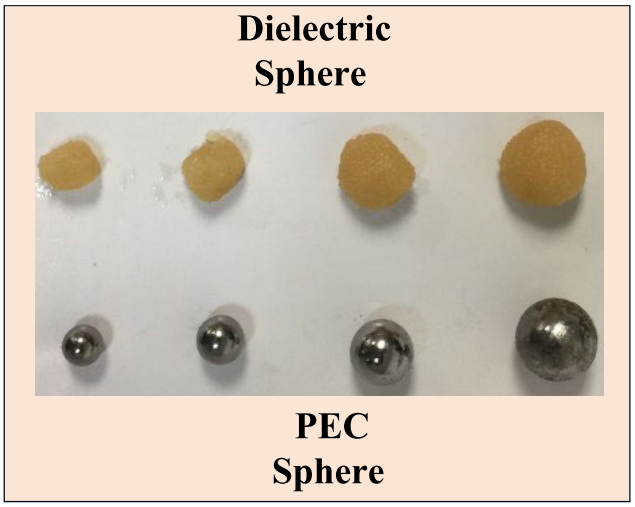

FIGURE 16. View of four different sizes ((7 mm,10 mm, 13 mm, and 16 mm) of high conductive (metallic spheres) and high dielectric spheres (oil gelatin mixture spheres).

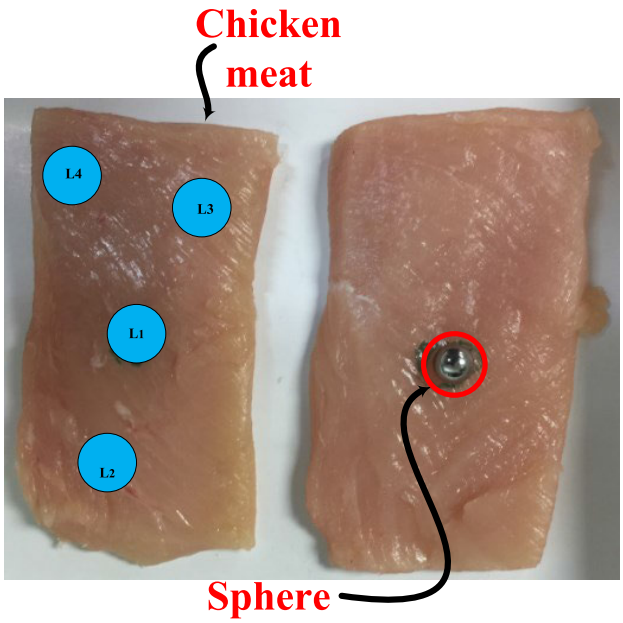

FIGURE 17. Measurement setup showing the process of allocating the tumor of radius 5 mm at various locations within the chicken meat.

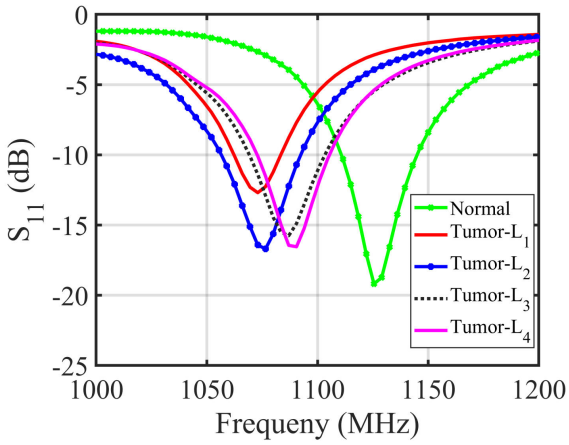

FIGURE 18. Showing the measuring results of the sensor's S_{11} magnitude response of the experimental studies that test the fabricated sensor array with chicken meat without a sphere and chicken meat containing a 10 mm high dielectric sphere placed at four different locations.

simulated with the abnormal breast phantom. In addition, the results show that changes in the current distribution are mainly due to loading the normal phantom with a tumor that has higher dielectric properties than the normal tissue, which affects the input impedance of the sensor causing a shift in the reflection coefficient of the sensor.

III. FABRICATION AND MEASUREMENT RESULTS

The experimental validation was performed with the same procedure as the simulation studies, investigating the sensitivity of the proposed array sensors for detecting different sizes of tumors inserted at various locations.

The measurement experiments consists of the sensor, a Vector Network Analyzer (VNA), metallic spheres, and tumors made of an oil and gelatin mixture with different diameter sizes, 7mm, 10 mm, 13 mm, and 16 mm, (mimicking tumors) [37], [38] and chicken meat as shown in Fig. 15 and Fig. 16 respectively.

We used the chicken meat in the experiment to test the feasibility of the proposed concept in an environment that have resemblance to female breast tissues. Although such environment is not identical to a realistic female breast, it serves the purpose since the main concept in the proposed detection technique is to detect the variation in the dielectric properties between regular breast tissue and tumors tissues. First, the proposed concept was proven numerically using a realistic breast and tumors tissues. However, experimental validation was carried out using chicken meat to mimic a female breast. Then, high dielectric and conductive spheres were inserted inside the meat which resembled tumors.

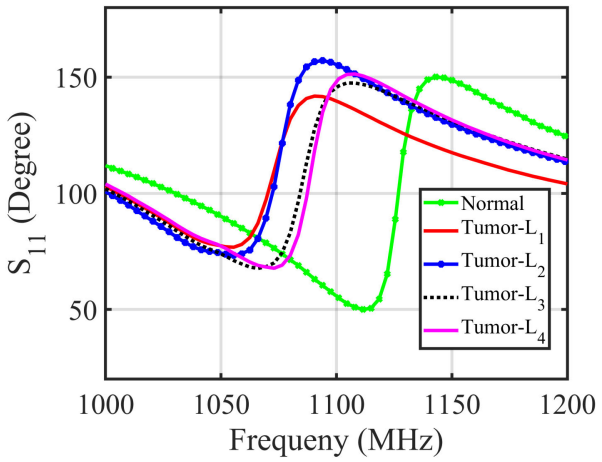

FIGURE 19. Showing the measuring results of the sensor's S_{11} phase response of the experimental studies that test the fabricated sensor array with chicken meat without a sphere and chicken meat containing a 10 mm high dielectric sphere placed at four different locations.

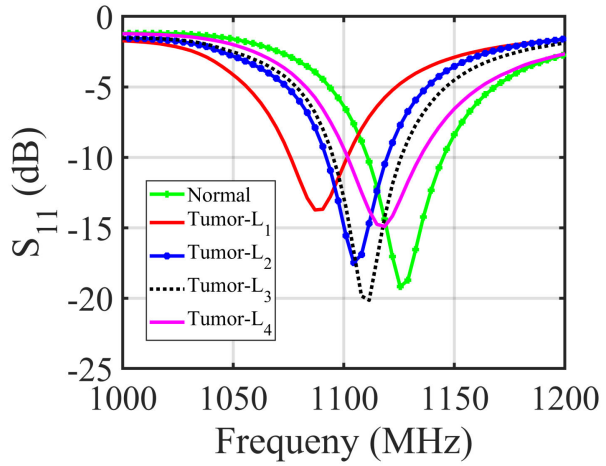

FIGURE 20. Showing the measuring results of the sensor's S_{11} magnitude response of the experimental studies that test the fabricated sensor array with chicken meat without a sphere and chicken meat containing a 10 mm high conductive metallic sphere placed at four different locations.

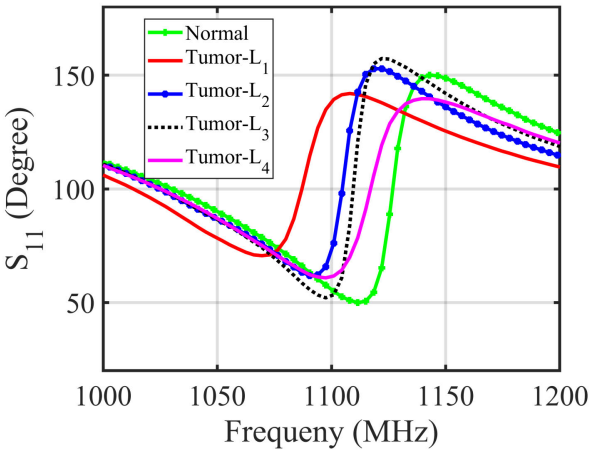

FIGURE 21. Showing the measuring results of the sensor's S_{11} phase response of the experimental studies that test the fabricated sensor array with chicken meat without a sphere and chicken meat containing a 10 mm high conductive metallic sphere placed at four different locations.

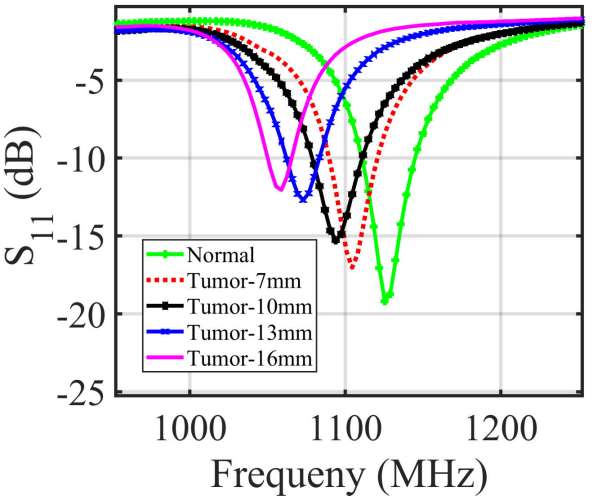

FIGURE 22. Showing the measuring results of the sensor's S_{11} magnitude response of the experimental studies that test the fabricated sensor array with chicken meat without a sphere and chicken meat containing four different sizes of high dielectric spheres (7 mm,10 mm, 13 mm, and 16 mm) placed at a single location.

The experimental setup is performed as the following: the fabricated sensor is placed in top of a Styrofoam box at a stand off distance of 5 mm away from the chicken meat which mimics an environment of a normal breast phantom model in the simulation studies and resembles female breast tissues as shown in Fig. 15.

In the first measurement scheme, the sensor response is measured in case of chicken meat without any inserted sphere (normal breast case). In the second case of the abnormal breast, two types of 10 mm diameter size tumors, highly dielectric and highly conductive, are inserted separately at four different locations inside the chicken meat that is divided into two pieces to ensure the tumor is placed in the specific location as shown in Fig. 17. Then, the sensor response is measured at each case of the different locations separately. The main purpose of performing this measurement study is to investigate the array sensor's ability to detect a tumor inserted at different locations without using the scanning methodology for detection.

The array sensor response from the experimental study of the two cases of inserting a 10 mm high dielectric and high conductive spheres at four different locations which mimic breast tumors are presented in figures Fig. 18 to Fig. 21. Figure 18 and Fig. 19 show the results of both magnitude and phase sensor response using a 10 mm high dielectric sphere at four different locations. Fig. 20 and Fig. 21 show the results of both magnitude and phase sensor response using a 10 mm high conductive sphere at four different locations. The results show that the sensor has high sensitivity for detecting both cases, high dielectric and high conducive, inserting spheres without utilizing mechanical scanning. However, the sensor sensitivity is higher when detecting the spheres located at the

TABLE 1. A comparative study of the proposed sensor dipole array with various state of the art published studies.

Reference	Frequency (GHz)	Size (mm)	Number of sensors	Sensor type	Using scanning	Image processing
[23]	2-12	22×22	8	square patch	Yes	Yes
[39]	3.9-19	30×30	2	patch	Yes	Yes
[16]	3-10	66×66	25	patch	Yes	Yes
[40]	1.6-10	60×70	25	circular patch	Yes	Yes
[27]	2.8-7	42×51	9	Vivaldi	Yes	Yes
[18]	1-10	24×45	2	monopole	Yes	Yes
[24]	5-10	42×73	1	Vivaldi	Yes	Yes
[37]	2.2-8	50×50	2	monopole	Yes	Yes
[41]	3.01–11.0	40×40	2	Vivaldi	Yes	Yes
[42]	3.2–14.0	16×71.5	4	patch	Yes	Yes
This work	**1-1.3**	**30×123**	4	**dipole**	**NO**	**NO**

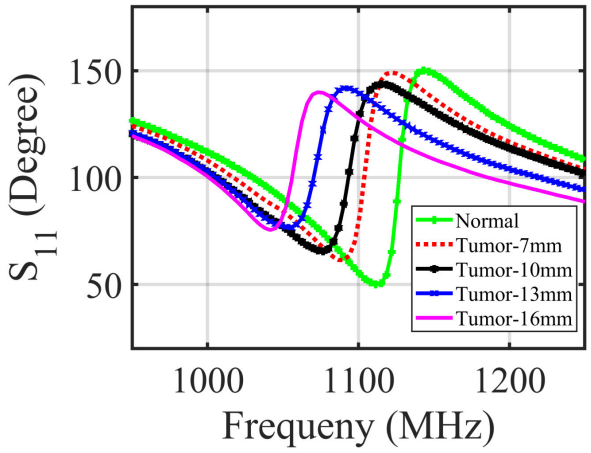

FIGURE 23. Showing the measuring results of the sensor's S_{11} phase response of the experimental studies that test the fabricated sensor array with chicken meat without a sphere and chicken meat containing four different sizes of high dielectric spheres (7 mm,10 mm, 13 mm, and 16 mm) placed at a single location.

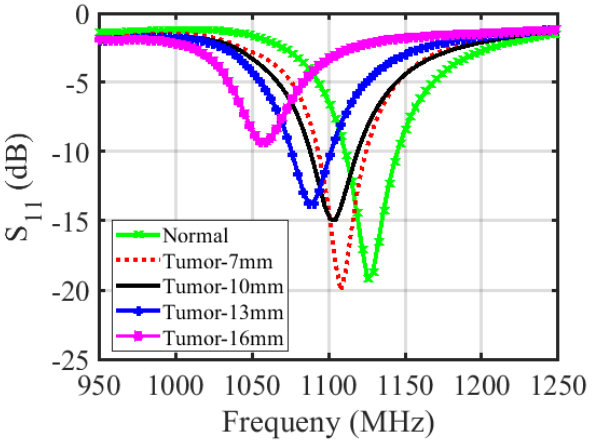

FIGURE 24. Showing the measuring results of the sensor's S_{11} magnitude response of the experimental studies that test the fabricated sensor array with chicken meat without a sphere and chicken meat containing four different sizes of high conductive metallic spheres (7 mm,10 mm, 13 mm, and 16 mm) placed at a single location.

sensor's center (L1) than other locations (L2, L3, and L4) where the spheres are placed off-center of the covered area of the sensor. Moreover, the sensor sensitivity is higher at detecting the high dielectric spheres than the high conductive metallic spheres.

Another experiment was performed to test the ability of the proposed sensor to detect various tumor sizes as shown in Fig. 16. In the experiment, the metallic spheres and tumors with various radii as indicated in the simulation were inserted inside the chicken meat. Here, the tumors and spheres where located in the same place one at a time. The response of the sensor was recorded for each case and compared to the original case having only chicken meat with no tumor. The magnitude and phase responses of different sizes tumors were analyzed and plotted as shown in Fig. 22 and Fig. 23. Figures 24 and Fig. 25 show the results of magnitude and phase responses of different metallic sizes of spheres. From the results, we can clearly see that as the tumor size increases, a higher frequency shift is experienced in both the magnitude and phase of the reflection coefficient.

$$\Delta Decision = S_{11}Right - S_{11}left \tag{1}$$

Table 1 compares the novelty and advantages of the proposed dipole array sensor introduced in this study with a number of state-of-the-art sensors that are based on the return loss for breast tumor detection presented in the literature.

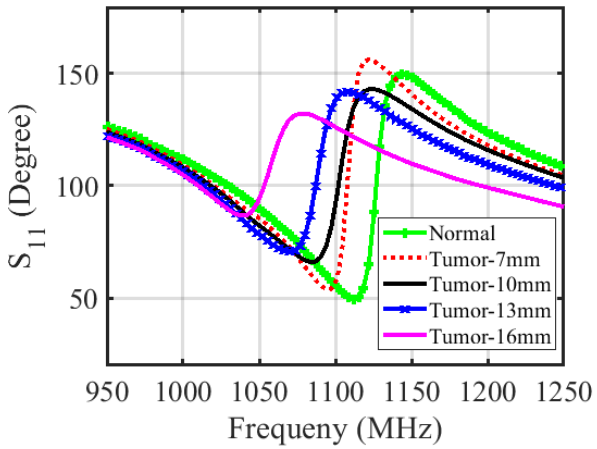

FIGURE 25. Showing the measuring results of the sensor's S_{11} phase response of the experimental studies that test the fabricated sensor array with chicken meat without a sphere and chicken meat containing four different sizes of high conductive metallic spheres (7 mm,10 mm, 13 mm, and 16 mm) placed at a single location.

Table 1 consists of six columns that show the operating frequency, size, number of elements, type of the antenna, the use of scanning technique and the use of image processing for detection. Comparing the proposed sensor with these state-of-the-art sensors, the proposed sensor has advantages including operating at lower frequencies which are suitable for higher penetrations and utilizing only one feed port which overcomes the challenges and complexity of the system. In addition, using the proposed sensor for detecting tumors without utilizing scanning and image processing techniques.

IV. CONCLUSION

A near-field dipole array sensor was presented for detecting breast tumors in the near-field at the microwave regime. The proposed sensor contains four electrically small dipoles that enhances the sensitivity area of the breast tissues under test. Simulation and experimental tests were performed to validate the proposed detection methodology using the proposed dipole sensor array. In the simulation section, two simulation studies were conducted to investigate the sensitivity of the proposed sensor for detecting breast tumors inserted at different locations inside a normal breast phantom with three different distances between the sensor and the breast phantom. Simulation results show that the proposed sensor is capable of detecting a breast tumor located any where inside the breast phantom by utilizing multiple sensor array which improved the sensitivity area of the sensor. Moreover, the closer the sensor to the breast phantom the more sensitive it is in detecting breast tumors. In the measurement study, two experimental studies were conducted using the fabricated sensor with chicken meat that mimics normal breast tissues with four different diameter sizes of metallic spheres and tumors made of an oil and gelatin mixture that resembles a breast tumor at various locations. Experimental results show that the fabricated sensor has higher sensitivity for detecting both types of tumors at the four proposed locations. In addition, the sensor is more sensitive to tumors made of an oil and gelatin mixture than the metallic spheres due to its higher response to dielectric material tissues than conductive material. Such dielectric sensitivity is a result of the construction configuration model of the proposed sensor which is based on the electrically small dipole resonators that concentrates the electric field in the gap between the two arms of each dipole and between the space between the four dipoles.

REFERENCES

[1] M. A. Aldhaeebi, K. Alzoubi, T. S. Almoneef, S. M. Bamatraf, H. Attia, and O. M. Ramahi, "Review of microwaves techniques for breast cancer detection," *Sensors*, vol. 20, no. 8, p. 2390, Apr. 2020.

[2] N. AlSawaftah, S. El-Abed, S. Dhou, and A. Zakaria, "Microwave imaging for early breast cancer detection: Current state, challenges, and future directions," *J. Imag.*, vol. 8, no. 5, p. 123, Apr. 2022.

[3] L. L. Wang, "Early diagnosis of breast cancer," *Sensors*, vol. 17, no. 7, p. 1572, 2017.

[4] M. Lazebnik, L. McCartney, D. Popovic, C. B. Watkins, M. J. Lindstrom, J. Harter, S. Sewall, A. Magliocco, J. H. Booske, M. Okoniewski, and S. C. Hagness, "A large-scale study of the ultrawideband microwave dielectric properties of normal breast tissue obtained from reduction surgeries," *Phys. Med. Biol.*, vol. 52, no. 10, pp. 2637–2656, May 2007.

[5] T. Sugitani, S.-I. Kubota, S.-I. Kuroki, K. Sogo, K. Arihiro, M. Okada, T. Kadoya, M. Hide, M. Oda, and T. Kikkawa, "Complex permittivities of breast tumor tissues obtained from cancer surgeries," *Appl. Phys. Lett.*, vol. 104, no. 25, Jun. 2014, Art. no. 253702.

[6] A. Martellosio, M. Pasian, M. Bozzi, L. Perregrini, A. Mazzanti, F. Svelto, P. E. Summers, G. Renne, L. Preda, and M. Bellomi, "Dielectric properties characterization from 0.5 to 50 GHz of breast cancer tissues," *IEEE Trans. Microw. Theory Techn.*, vol. 65, no. 3, pp. 998–1011, Mar. 2017.

[7] L. Wang, "Microwave sensors for breast cancer detection," *Sensors*, vol. 18, no. 2, p. 655, Feb. 2018.

[8] A. Attaran, W. B. Handler, and B. A. Chronik, "2 mm radius loop antenna and linear active balun for near field measurement of magnetic field in MRI-conditional testing of medical devices," *IEEE Trans. Electromagn. Compat.*, vol. 62, no. 1, pp. 186–193, Feb. 2020.

[9] J. Radder, M.-K. Woo, P.-F. Van de Moortele, G. Metzger, A. Ertürk, J. Strupp, K. Ugurbil, and G. Adriany, "Optimization and simulation of a 16-channel loop and dipole array for head MRI applications at 10.5 Tesla," in *Proc. Int. Conf. Electromagn. Adv. Appl. (ICEAA)*, Sep. 2017, pp. 1828–1831.

[10] A. Syed, N. Sobahi, M. Sheikh, R. Mittra, and H. Rmili, "Modified 16-quasi log periodic antenna array for microwave imaging of breast cancer detection," *Appl. Sci.*, vol. 12, no. 1, p. 147, Dec. 2021.

[11] F.-E. Zerrad, M. Taouzari, E. M. Makroum, J. E. Aoufi, S. D. Qanadli, M. Karaaslan, A. J. A. Al-Gburi, and Z. Zakaria, "Microwave imaging approach for breast cancer detection using a tapered slot antenna loaded with parasitic components," *Materials*, vol. 16, no. 4, p. 1496, Feb. 2023.

[12] M. Toolabi, M. Khatir, M. Naser-Moghadasi, and N. Amiri, "Vivaldi antenna for early cancer detection based on THz spectroscopy: Comparison between response of breast and skin cancer," *Optik*, vol. 273, Feb. 2023, Art. no. 170440.

[13] L. A. El Vadel, D. B. Konditi, and F. M. Mbango, "A miniaturized antenna for breast cancer detection at the 5.72–5.82 GHz ISM band based on the DGS technique," *Prog. Electromagnetics Res. B*, vol. 98, pp. 1–19, 2023.

[14] H. M. E. Misilmani, T. Naous, S. K. A. Khatib, and K. Y. Kabalan, "A survey on antenna designs for breast cancer detection using microwave imaging," *IEEE Access*, vol. 8, pp. 102570–102594, 2020.

[15] M. Klemm, I. J. Craddock, J. A. Leendertz, A. Preece, and R. Benjamin, "Radar-based breast cancer detection using a hemispherical antenna array—Experimental results," *IEEE Trans. Antennas Propag.*, vol. 57, no. 6, pp. 1692–1704, Jun. 2009.

[16] M. Z. Mahmud, M. T. Islam, N. Misran, S. Kibria, and M. Samsuzzaman, "Microwave imaging for breast tumor detection using uniplanar AMC based CPW-fed microstrip antenna," *IEEE Access*, vol. 6, pp. 44763–44775, 2018.

[17] M. T. Islam, M. Z. Mahmud, N. Misran, J.-I. Takada, and M. Cho, "Microwave breast phantom measurement system with compact side slotted directional antenna," *IEEE Access*, vol. 5, pp. 5321–5330, 2017.
[18] D. N. Elsheakh, R. A. Mohamed, O. M. Fahmy, K. Ezzat, and A. R. Eldamak, "Complete breast cancer detection and monitoring system by using microwave textile based antenna sensors," *Biosensors*, vol. 13, no. 1, p. 87, Jan. 2023.
[19] P. K. Rao, A. R. Yadav, and R. Mishra, "AMC-based antenna sensor for breast tumors detection," *Int. J. Microw. Wireless Technol.*, vol. 13, no. 9, pp. 954–961, Nov. 2021.
[20] M. A. Aldhaeebi, T. S. Almoneef, A. Ali, Z. Ren, and O. M. Ramahi, "Near field breast tumor detection using ultra-narrow band probe with machine learning techniques," *Sci. Rep.*, vol. 8, no. 1, pp. 1–16, Aug. 2018.
[21] M. A. Aldhaeebi, T. S. Almoneef, H. Attia, and O. M. Ramahi, "Electrically small magnetic probe with PCA for near-field microwave breast tumors detection," *Prog. Electromagn. Res. M*, vol. 84, pp. 177–186, 2019.
[22] N. V. Shahmirzadi, V. Tyagi, J. Nguyen, R. Kazemivala, N. K. Nikolova, and C.-H. Chen, "Planar array of UWB active slot antennas for microwave imaging of the breast," *IEEE Trans. Antennas Propag.*, vol. 71, no. 4, pp. 2946–2957, Apr. 2023.
[23] M. Alibakhshikenari, B. S. Virdee, P. Shukla, N. O. Parchin, L. Azpilicueta, C. H. See, R. A. Abd-Alhameed, F. Falcone, I. Huynen, T. A. Denidni, and E. Limiti, "Metamaterial-inspired antenna array for application in microwave breast imaging systems for tumor detection," *IEEE Access*, vol. 8, pp. 174667–174678, 2020.
[24] H. Zhang, "Microwave imaging for breast cancer detection: The discrimination of breast lesion morphology," *IEEE Access*, vol. 8, pp. 107103–107111, 2020.
[25] M. T. Islam, M. Samsuzzaman, S. Kibria, and M. T. Islam, "Experimental breast phantoms for estimation of breast tumor using microwave imaging systems," *IEEE Access*, vol. 6, pp. 78587–78597, 2018.
[26] M. T. Islam, M. T. Islam, M. Samsuzzaman, H. Arshad, and H. Rmili, "Metamaterial loaded nine high gain Vivaldi antennas array for microwave breast imaging application," *IEEE Access*, vol. 8, pp. 227678–227689, 2020.
[27] M. T. Islam, M. Z. Mahmud, M. T. Islam, S. Kibria, and M. Samsuzzaman, "A low cost and portable microwave imaging system for breast tumor detection using UWB directional antenna array," *Sci. Rep.*, vol. 9, no. 1, pp. 1–13, Oct. 2019.
[28] A. Hossain, M. T. Islam, M. T. Islam, M. E. H. Chowdhury, H. Rmili, and M. Samsuzzaman, "A planar ultrawideband patch antenna array for microwave breast tumor detection," *Materials*, vol. 13, no. 21, p. 4918, Nov. 2020.
[29] M. A. Aldhaeebi, T. S. Almoneef, H. Attia, and O. M. Ramahi, "Near-field microwave loop array sensor for breast tumor detection," *IEEE Sensors J.*, vol. 19, no. 24, pp. 11867–11872, Dec. 2019.
[30] V. Gazhonova, *3D Automated Breast Volume Sonography: A Practical Guide*. Cham, Switzerland: Springer, 2016.
[31] J.-H. Chen, S. Chan, D.-C. Yeh, P. T. Fwu, M. Lin, and M.-Y. Su, "Response of bilateral breasts to the endogenous hormonal fluctuation in a menstrual cycle evaluated using 3D MRI," *Magn. Reson. Imag.*, vol. 31, no. 4, pp. 538–544, May 2013.
[32] CST. (Sep. 2023). *Computer Simulation Technology*. CST Computer Simulation Technology Ag. [Online]. Available: http://www.CST.com
[33] UWCEM. (Aug. 2017). *Breast Phantom Repository@ONLINE*. [Online]. Available: http://uwcem.ece.wisc.edu/phantomRepository.html
[34] E. Zastrow, S. Davis, M. Lazebnik, F. Kelcz, B. Van Veem, and S. Hagness, "Database of 3D grid-based numerical breast phantoms for use in computational electromagnetics simulations," Dept. Electr. Comput. Eng., Univ. Wisconsin-Madison, Madison, WI, USA, Tech. Rep. 062204 ACR, 2008.
[35] E. Zastrow, S. K. Davis, M. Lazebnik, F. Kelcz, B. D. Van Veen, and S. C. Hagness, "Development of anatomically realistic numerical breast phantoms with accurate dielectric properties for modeling microwave interactions with the human breast," *IEEE Trans. Biomed. Eng.*, vol. 55, no. 12, pp. 2792–2800, Dec. 2008.
[36] A. C. Society. (2023). *Cancer Facts and Figures 2023*. [Online]. Available: https://www.cancer.org/cancer/types/breast-cancer/understanding-a-breast-cancer-diagnosis/stages-of-breast-cancer.html
[37] D. M. Elsheakh, S. A. Alsherif, and A. R. Eldamak, "Textile monopole sensors for breast cancer detection," *Telecommun. Syst.*, vol. 82, no. 3, pp. 363–379, Mar. 2023.
[38] M. Lazebnik, E. L. Madsen, G. R. Frank, and S. C. Hagness, "Tissue-mimicking phantom materials for narrowband and ultrawideband microwave applications," *Phys. Med. Biol.*, vol. 50, no. 18, pp. 4245–4258, Sep. 2005.
[39] H. Li, H. Zhang, Y. Kong, and C. Zhou, "Flexible dual-polarized UWB antenna sensors for breast tumor detection," *IEEE Sensors J.*, vol. 22, no. 13, pp. 13648–13658, Jul. 2022.
[40] A. AlOmairi and D. Ç. Atilla, "Ultra-wide-band microstrip patch antenna design for breast cancer detection," vol. 22, no. 1, pp. 41–51, 2022.
[41] M. T. Islam, M. Samsuzzaman, M. T. Islam, S. Kibria, and M. J. Singh, "A homogeneous breast phantom measurement system with an improved modified microwave imaging antenna sensor," *Sensors*, vol. 18, no. 9, p. 2962, Sep. 2018.
[42] P. K. Rao and R. Mishra, "Elliptical shape flexible MIMO antenna with high isolation for breast cancer detection application," *IETE J. Res.*, vol. 69, no. 1, pp. 325–333, 2020.

MAGED A. ALDHAEEBI (Member, IEEE) received the B.S. degree in electrical and computer engineering from Hadhramaut University, Al-Mukalla, Hadhramaut, Yemen, in 2009, the M.A.Sc. degree in electrical and computer engineering from King Saud University, Riyadh, Saudi Arabia, in 2014, and the Ph.D. degree in electrical and computer engineering from the University of Waterloo, Waterloo, ON, Canada, in 2020. He is currently an Assistant Professor with the Department of Electrical Engineering, Prince Sattam bin Abdulaziz University. He has authored or coauthored more than 30 refereed journal articles and conference papers. His research interests include biomedical engineering, breast and brain tumors imaging and detection, intelligent microwaves-based modalities for breast cancer detection, artificial intelligence, antenna theory, metamaterials and their wide range applications, metamaterial absorbers, electrically small resonators, rectennas, microwave sensors, electromagnetic energy harvesting, and machine learning for electromagnetic biomedical applications.

THAMER S. ALMONEEF (Member, IEEE) received the B.S. degree in electrical and computer engineering from Dalhousie University, Halifax, NS, Canada, in 2009, and the M.A.Sc. and Ph.D. degrees in electrical and computer engineering from the University of Waterloo, Waterloo, ON, Canada, in 2012 and 2017, respectively. In 2012, he was appointed as a Lecturer and was granted a Scholarship from Prince Sattam bin Abdulaziz University, Al-Kharj, Saudi Arabia, to pursue his Ph.D. degree studies. He is currently an Associate Professor with the Department of Electrical and Computer Engineering, Prince Sattam bin Abdulaziz University. He has authored or coauthored more than 35 refereed journal articles and conference papers. His research interests include antenna theory, metamaterials and their wide range applications, metamaterial absorbers, electrically small resonators, rectennas, microwave sensors and imagers, electromagnetic energy harvesting, and renewable energy.